Modular Autonomous Electric Vehicle Scheduling for Customized On-Demand Bus Services

Rongge Guo, Wei Guan, Mauro Vallati, and Wenyi Zhang

***Abstract*— The emerging customized bus system based on modular autonomous electric vehicles (MAEVs) shows tremendous potential to improve the mobility, accessibility and environmental friendliness of a public transport system. However, the existing studies in this area almost focus on human-driven vehicles which face some striking limitations (e.g., restricted crew scheduling and fixed vehicle capacity) and can weaken the overall benefits. This paper proposes a two-phase optimization procedure to fully unleash the potential of MAEVs by leveraging the strengths of MAEVs, including automatic allocation and charging of modules. In the *first* phase, a mixed integer programming model is established in the space-time-state framework to jointly optimize the MAEV routing and charging, passenger-to-vehicle assignment and vehicle capacity management for reserved passengers. A Lagrangian relaxation algorithm is developed to solve the model efficiently. In the *second* phase, three dispatching strategies are designed and optimized by a dynamic dispatching procedure to properly adapt the operation of MAEVs to emerging travel demands. A case study conducted on a major urban area of Beijing, China, demonstrates the high efficiency of the MAEV adoption in terms of resource utilization and environmental friendliness across a range of travel demand distributions, vehicle supply and module capacity scenarios.**

***Index Terms*— Customized bus, modular autonomous electric vehicle, space-time-state network, Lagrangian relaxation, dynamic dispatching.**

I. Introduction

THE customized bus (CB) system is an emerging demand-responsive transit (DRT) service that aims to improve the punctuality and serviceability of the public transit (PT) system [1]. It offers great accessibility with non-transfer and door-to-door service to passengers with similar travel requests in both space and time, or personalized requirements [2]. The CB system operates with flexible routes, timetables, and schedules, based on the time-varying travel demands. Practical experience has acknowledged that CB can provide an effective and green alternative to private cars and conventional buses [3].

Routinely, a CB system plans the service according to passengers' travel requirements submitted in advance via dedicated online booking. The CB service regarding routes, timetables, vehicles, and crew schedules designed for given static demands are then fixed for the service duration, which is known as the first phase. The work of [4] first introduced a CB route planning framework, which was then extended to consider the timetable design and passenger choice behaviors when dealing with the clustering travel demands [5]. As travel demands are assumed to be known and static beforehand, some studies treat the CB service design problem as a generalized extension of the vehicle routing problem with pick-up and delivery [6]. They put forward the exclusive decision variable for modeling passenger-to-vehicle (P2V) assignment and extended the CB design problem to address the scenario with the travel time dependency and path flexibility [7].

In practice, however, many travel requests are likely to be submitted in almost real-time, after the first phase has been completed and shortly before the actual need for the service. Those emerging requests pose a challenge for maintaining the punctuality and effectiveness of the CB system. The conventional addressing method is to either update initial routes generated for reserved requests or dispatch new vehicles [8], [9]. Existing approaches for CB systems usually consider human-driven vehicles (HVs), which may hinder the ability to cope with emerging time-sensitive requests. This is due to the crew schedule, which may not allow accommodating the potentially significant detour time required to serve such requests. Furthermore, HVs have fixed capacity, which may result in lower vehicle loads and significant capacity waste due to a lack of flexibility in the presence of real-time requests.

The innovative autonomous electric vehicles (AEVs) technology can support urban mobility and reduce the carbon footprint of on-demand transit systems [10]. A major benefit lies in the fact that AEVs can achieve automated allocation, improve charging management and remove range anxiety, especially in car sharing and PT [11], [12]. Specifically, the integration of AEVs and PT provides a powerful platform for delivering efficient on-demand transportation services: [13] successfully implemented autonomous technology to offer on-demand services to fixed-route buses dealing with the first/last mile problem; [14] concluded that autonomous mobility-on-demand transit system could balance the vehicle distribution. Another remarkable feature is that AEVs can be treated as modular autonomous electric vehicle (MAEV) units,

Manuscript received 16 October 2022; revised 24 February 2023 and 14 April 2023; accepted 24 April 2023. Date of publication 9 May 2023; date of current version 30 August 2023. This work was supported in part by the National Natural Science Foundation of China under Grant 72271018 and Grant 91746201 and in part by the UK Research and Innovation (UKRI) Future Leaders Fellowship under Grant MR/T041196/1. The Associate Editor for this article was Z. Ma. *(Corresponding author: Wenyi Zhang.)*

Rongge Guo and Mauro Vallati are with the School of Computing and Engineering, University of Huddersfield, HD1 4QA Huddersfield, U.K.

Wei Guan and Wenyi Zhang are with the Key Laboratory of Transport Industry of Big Data Application Technologies for Comprehensive Transport, Ministry of Transport, Beijing Jiaotong University, Beijing 100044, China (e-mail: wyzhang@bjtu.edu.cn).

This article has supplementary downloadable material available at https://doi.org/10.1109/TITS.2023.3271690, provided by the authors.

Digital Object Identifier 10.1109/TITS.2023.3271690

This work is licensed under a Creative Commons Attribution 4.0 License. For more information, see https://creativecommons.org/licenses/by/4.0/

which are allowed to assemble or disassemble into varying capacities while traveling on roads [15]. Such a novel concept enables high capacity flexibility for accommodating real-time requests, and provides the potential to improve accessibility and reliability while enhancing capacity utilization rate and operational efficiency in PT systems [16]. Some researchers have explored the benefits of modularity in bus routing and scheduling when dealing with time-dependent travel requests [17], [18]. Recently, a few studies have investigated the use of modular vehicles in flexible transit service: [19] extended modular transit into the first- and last-mile problem; [20], [21] introduced the hybrid transit service (fixed and flexible routes) to improve service quality for door-to-door services.

With the aim of fully nurturing the potential of a CB system, this paper provides a novel scheduling methodology for the modular autonomous electric customized bus (MAECB) system. We make threefold contributions:

- First, we define the MAECB system operation, where the emerging MAEV technology is integrated to deal with heterogeneous travel requests. The new CB scenario can address the joint optimization of routing, scheduling, charging, P2V assignment, and dynamic capacity management, which can fully accommodate the space- and time-varying travel requests.
- Second, we introduce a two-phase optimization procedure to adequately address the reserved and emerging travel demands. A mixed integer programming model is developed in the space-time-state framework to formulate the problem of the first phase. A Lagrangian relaxation algorithm is proposed to solve the model, where the complex problem is decomposed into an electric vehicle routing problem, a P2V assignment problem, and a module assembling problem. Three dispatching strategies, which are optimized by a dynamic dispatching procedure, are introduced to re-optimize the service in the second phase. The re-optimal plan is dynamically adapted to travel demands arising in multiple periods.
- Third, we perform extensive numerical experiments on large-scale real-world instances, which yields valuable insights into the capabilities of the proposed MAECB system. We empirically demonstrate that i) the resulting MAECB system is more effective and efficient than the HV-based CB system, particularly in terms of vehicle usage and operating cost; and ii) the adoption of MAEV technology can significantly reduce environmental pollution and energy consumption.

To better position and contextualize this work, Table I presents an overview of the existing literature in this field.

TABLE I
OVERVIEW OF RELATED WORK ON CB SYSTEMS

Study	Request	Vehicle	Objective	Decision variables	Algorithm
[6]	Reserved	HV	Operating costs	Route,timetable, assignment	LRH
[5]	Reserved	HV	Profits	Stop,timetable, route, passenger choice	DP
[8]	Reserved, emerging	HV	Profits	Route,schedule, assignment	B&B, DP
[22]	Reserved, emerging	HV	Travel time, operating costs	Routes, assignments	NSGA-II
[23]	Reserved	MAV	System costs	Route,vehicle type, assignment	PSO
[24]	Reserved, emerging	AEV	Operating costs	Route,charging, assignment	ALNS
This study	**Reserved, emerging**	**MAEV**	**Operating costs**	**Route,schedule, assignment,capacity, charging**	**LRH, DDP**

Note: LRH=Lagrangian relaxation heuristic; B&B=Branch and bound; DP=Dynamic programming; NSGA-II=Non-dominated Sorting Genetic Algorithm II; PSO=Particle swarm optimization; ALNS=Adaptive large neighborhood search; DDP=Dynamic dispatching procedure

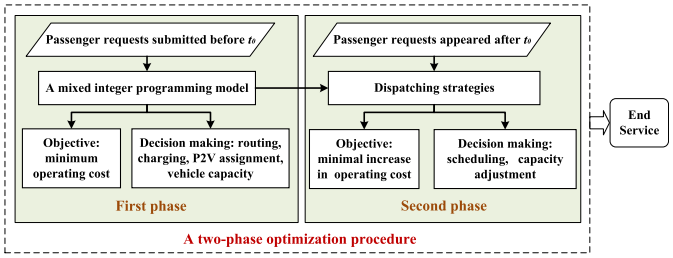

Fig. 1. The two-phase optimization procedure of the MAECB service.

II. PROBLEM DESCRIPTION

This section provides a formal description of the on-demand MAECB scheduling problem. The problem can be naturally presented as a two-phase optimization problem, as shown in Fig. 1. The first phase aims to plan the service for passenger groups who book CBs beforehand. The second phase re-optimizes the existing service through dynamic vehicle scheduling, based on emerging travel requests.

Fig. 2 exemplifies the temporal nature of the considered problem. The on-demand MAECB scheduling problem can be characterized to serve passenger groups $P = \{p_1, p_2, \ldots, p_n\}$ submitted ($\theta_n < t_0$, θ_n is the submitted time for passenger group p_n) before time t_0 and the groups $P' = \{p_{(n+1)}, p_{(n+2)}, \ldots, p_{(n+m)}\}$ that dynamically arrive ($\theta_{n+1} > t_0$) through the finite horizon $T = [t_0, |T|]$. Each passenger group represents multiple passengers with the same travel plan, characterized by pick-up and drop-off points (r, s), corresponding preferred time windows $([ear_r, lat_r], [ear_s, lat_s])$, and quantity Num_p. At every timestamp $t\,(t_0 \le t \le T)$, group $p \in P \cup P'$ can be in one of four states $\alpha_p(t) \in \{1, 2, 3, 4\}$, denoting unassigned, assigned, in-vehicle and served, respectively. These four states correspond to four mutually exclusive subsets of passenger groups. The unassigned groups $P_U(t) = \{P \cup P' \mid \alpha_p(t) = 1\}$ have made a request but have not yet been assigned. The assigned groups $P_A(t) = \{P \cup P' \mid \alpha_p(t) = 2\}$ have been assigned but not yet picked up. The in-vehicle groups $P_I(t) = \{P \cup P' \mid \alpha_p(t) = 3\}$ have been picked up, while the served groups $P_S(t) = \{P \cup P' \mid \alpha_p(t) = 4\}$ have arrived at their destinations.

As shown in Fig. 2, the system has full information about reserved travel requests at time t_0, and allocates these groups

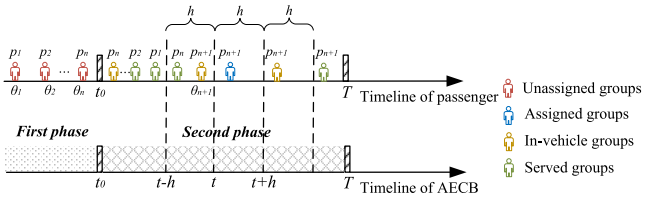

Fig. 2. Timeline of MAECB system.

to vehicles. This process corresponds to the *first* phase. After t_0 ($t > t_0$), emerging travel demands can be received at every time interval h. At t, the system has full information about generated passenger groups before t. Therefore, the system re-plans the MAECB service for new requests $P_U(t)$, until the states of all passenger groups turn to served $\alpha_p(t) = 4$ and t is greater than T. This process of assessing new requests at every h and adapting the original plan accordingly corresponds to the *second* phase. The inter-operation time interval h is an adjustable parameter of which the value depends on various external factors.

To serve passengers, here we consider a homogeneous AECB module fleet $M = \{1, 2, \ldots, |M|\}$. At timestamp t, each module has a physical location $posV_m(t)$ and a state $\beta_m(t)$. The module $m \in M$ can be in one of three states $\beta_m(t) \in \{1, 2, 3\}$ differentiating between modules that are idle $M_I(t) = \{M \mid \beta_m(t) = 1\}$, en-route $M_E(t) = \{M \mid \beta_m(t) = 2\}$, and charging $M_C(t) = \{M \mid \beta_m(t) = 3\}$, respectively. The idle state implies that a module is in a depot or a charging station, which has been fully charged and can be activated for service. The en-route state means that a module has already left the depot for serving passengers. The charging state indicates that a module is recharging the battery at a charging station. If the remaining electricity of a module is estimated to be below the minimum threshold e_{min} before reaching the next vertex (including pick-up and drop-off points, and the nearest charging station), then it must go to the nearest charging station and get fully charged with a constant recharging rate g. At timestamp t_0, modules are all in the idle state $m \in M_I (M_I = \{M \mid \beta_m(t) = 1\})$, and are fully charged at depots.

A key point of the MAECB service is that modules can be assembled at depots and/or disassembled on roads into a set of AECBs ($K = \{1, 2, \ldots, |K|\}$) with varying capacities, to serve fluctuating travel demands. The capacity cap^w of an AECB varies against the vehicle type $w (w \in W)$ which ultimately depends on the number of assembling modules. However, we do not consider assembling on roads, as the movement of a vehicle will be heavily affected by the assembling modules with unequal remaining energy states. Further, each AECB $k \in K$ has a physical location $posV_k(t)$ and one of three states $\beta_k(t) \in \{1, 2, 3\}$ at t, which is associated with $posV_m(t)$ and $\beta_m(t)$ of modules.

Fig. 3 gives an example to illustrate the assembling and disassembling operations. In the first phase t_0, idle modules m_1, m_2 and m_3 are assembled into vehicle k_1 for serving passenger group 1. In the second phase, a new travel request OD2 emerges at t. After dropping off the passengers of

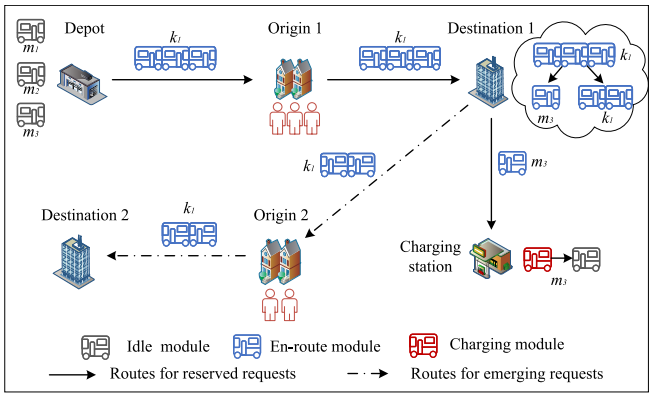

Fig. 3. Assembling and disassembling of AECB modules.

OD1, the en-route vehicle k_1 is disassembled into m_3 and k_1, according to the passenger quantity of OD2; then, k_1 is scheduled to serve the new passengers, while m_3 moves to charging station for recharging. After finishing recharging, m_3 turns to be idle state.

III. MAECB Service Plan for the First Phase

In this section, a space-time-state network-based model is formulated to optimize the operation of MAECB for the reserved travel demands in the first phase. A Lagrangian relaxation algorithm is developed to solve the model.

A. Mathematical Model

To facilitate handling the complex temporal-spatial constraints and relations in the route planning of the first phase, we adopt the discrete space-time-state modeling framework to construct a CB service network with three dimensions, including the space, time and state dimensions [25].

Consider a service network $G = (V, A)$, where the vertices are depicted by the space-time-state tuple (i, t, e), indicating that the AECB k maintains the state e with the cumulative number of remaining electricity at vertex i at time t. An arc $(i, j, t, t', e, e') \in A$ signifies the directed path from vertex (i, t, e) to vertex (j, t', e'), and it indicates that k travels through the arc (i, j) during the time duration (t, t') with the remaining energy change $(e \to e')$. The state e indicates the remaining electricity which must be beyond the minimum threshold e_{min}, otherwise, the AECB must be recharged. The time horizon is discretized into a series of 1-min-width time intervals. The use of a space-time-state network model makes it convenient to embed a set of constraints (including those regarding time window, electricity state and charging) into the algorithm to remove the infeasible arcs and prune the search space efficiently [26]. Table II lists the sets, indices, parameters and variables used in the model.

The basic assumptions of the model are the following: (1) AECBs begin and end their routes at depots; (2) each AECB leaves the depots and charging stations with a full charge, and the power consumption rate is a constant and calculated per travel distance; (3) If the remaining electricity is estimated to be below the given threshold before reaching the next vertex, the AECB will get fully charged at the nearest charging

TABLE II
MODEL NOTATIONS

Symbol	Definition
Sets and indices	
V	Set of space-time-state vertices
S	Set of pick-up and drop-off points
O	Set of depots
F	Set of charging stations
A	Set of space-time-state traveling arcs
$A^r(p)$	Set of pick-up space-time-state arcs whose head vertices belong to $\delta^r(p)$
$A^s(p)$	Set of drop-off space-time-state arcs whose tail vertices belong to $\delta^s(p)$
Ψ_o^k	Set of departure arcs for depots
M	Set of AECB modules, $M = M_I \cup M_E \cup M_C$
M_I, M_E, M_C	Set of idle, en-route and charging AECB modules
K	Set of AECB vehicles, $K = K_I \cup K_E \cup K_C$
K_I, K_E, K_C	Set of idle, en-route and charging AECB vehicles
W	Set of AECB vehicle types
P	Set of passenger groups
P_U, P_A, P_I, P_S	Set of unassigned, assigned, in-vehicle and served passenger groups
E	Set of cumulative electricity states of AECBs
(i,t,e)	Indices of space-time-state vertices
(i,j,t,t',e,e')	Indices of space-time-state arcs
w	Indices of vehicle types for AECBs
a	Abbreviation index of arc
Parameters	
$c_{i,j,t,t',e,e'}$	Travel cost on arc (i,j,t,t',e,e')
c^w	Unit module departure cost if the module is assembled into w-type AECB
$d_{i,j}$	Distance between vertex i and j
$t_{i,j}$	Travel time between vertex i and j
cap	AECB module capacity
cap^w	Vehicle capacity of w-type AECB
Num_p	Passenger number of group p
g	Recharging rate
h	Charge consumption rate related to traveled distance
e_{min}	Minimum threshold of remaining electricity
e_o	Full electricity
$\delta^r(p)$,$\delta^s(p)$	Paired space-time windows of p
DeT^k, ArT^k	Earliest departure time and latest arrival time of k
$Load^w$	Minimum load requirement for AECB with type w
Decision variables	
$x^{k,w}_{i,j,t,t',e,e'}$	Equal to 1 if arc (i,j,t,t',e,e') is passed through by AECB k with vehicle type w
$z^{k,m,w}$	Equal to 1 if AECB k is assembled by the module m
$y_p^{k,w}$	Equal to 1 if group p is served by k with type w

station and the recharging rate is constant; (4) modules are homogeneous, and can be assembled or disassembled into capacity-flexible AECB vehicles; (5) passenger groups should be served within their preferred time windows.

The MAECB service plan for the first phase aims to minimize the operating costs, including total traveling costs and departure costs. The objective function can then be stated as expression (1), subject to constraints (2)–(10).

$$min\ C = \sum_{(i,j,t,t',e,e')\in A} \sum_{k\in K_I} \sum_{w\in W} w c_{i,j,t,t',e,e'} x^{k,w}_{i,j,t,t',e,e'} + \sum_{k\in K_I} \sum_{m\in M_I} \sum_{w\in W} c^w z^{k,m,w} \tag{1}$$

$$\text{s.t.} \sum_{(i,j,t,t',e,e')\in A} x^{k,w}_{i,j,t,t',e,e'} - \sum_{(j,i,t',t,e',e)\in A} x^{k,w}_{j,i,t',t,e',e} = \begin{cases} 1 & i \in O, t = DeT^K, e = e_o, \\ -1 & i \in O, t = ArT^K, e \in E, \\ 0 & \text{otherwise}, \end{cases} \quad k \in K_I, w \in W \tag{2}$$

$$\sum_{k\in K_I} \sum_{w\in W} y_p^{k,w} = 1,\ p \in P_U \tag{3}$$

$$y_p^{k,w} \le \sum_{(i,j,t,t',e,e')\in A^r(p)} x^{k,w}_{i,j,t,t',e,e'},\quad p \in P_U, k \in K_I, w \in W \tag{4}$$

$$y_p^{k,w} \le \sum_{(i,j,t,t',e,e')\in A^s(p)} x^{k,w}_{i,j,t,t',e,e'},\quad p \in P_U, k \in K_I, w \in W \tag{5}$$

$$\sum_{p\in P_U} y_p^{k,w} Num_p \le cap^w,\ k \in K_I, w \in W \tag{6}$$

$$\sum_{p\in P_U} y_p^{k,w} Num_p \ge Load^w,\ k \in K_I, w \in W \tag{7}$$

$$\sum_{m\in M_I} z^{k,m,w} = w x^{k,w}_{i,j,t,t',e,e'},\quad (i,j,t,t',e,e') \in \Psi_o^k, k \in K_I, w \in W \tag{8}$$

$$\sum_{k\in K_I} \sum_{w\in W} z^{k,m,w} \le 1,\ m \in M_I \tag{9}$$

$$\sum_{k\in K_I} \sum_{m\in M_I} \sum_{w\in W} z^{k,m,w} \le |M| \tag{10}$$

Constraints (2) ensure the balance of AECB flow at the depot, which shows that each AECB must originate from and terminate at the designated depot. Constraints (3) depict that each passenger group must be served. Constraints (4) and (5) show that if group p is assigned to an AECB, the vehicle must visit both the pick-up and drop-off points of p and satisfy the time window constraints herein. Constraints (6) are vehicle capacity constraints. Constraints (7) formulate the minimum load requirement for activating an idle vehicle. Constraints (8)-(10) capture the modular features. Constraints (8) show that the type of an AECB is decided by the number of modules assembled to this vehicle. Constraints (9) represent that a module can be activated or not, depending on the cost effectiveness. Constraints (10) define the quantitative upper bound of the applicable modules.

B. Lagrangian Relaxation Heuristic Algorithm

The first-phase problem can be viewed as a variant of the vehicle routing problem which has been proven to be computationally NP-hard. In this study, we propose a Lagrangian relaxation heuristic (LRH) algorithm to solve it. In the literature, the LRH has shown desirable performance in solving similar high-dimensional and large-scale combinatorial optimization problems [27].

1) Lagrangian Relaxation and Decomposition: It is worth noting that a solution of the MAECB service involves three types of decisions: (i) how AECBs travel in the network; (ii) how to assign a passenger to an AECB; and (iii) how to assemble or disassemble modules. In the model, Constraints (4), (5) and (8) involve the coupling of decision variables $x_a^{k,w}$ and $y_p^{k,w}$, $x_a^{k,w}$ and $z^{k,m,w}$, which can be viewed as the primarily hard constraints and relaxed into the objective function. By relaxing the three constraints and associating them with multipliers $\lambda_p^{k,w}$, $\beta_p^{k,w}$ and $\pi_a^{k,w}$, we obtain the

relaxed model of the first phase as follows:

$$\begin{aligned} min\ L(\lambda,\beta,\pi) = & \sum_{a\in A}\sum_{k\in K_I}\sum_{w\in W} wc_a x_a^{k,w} \\ & + \sum_{k\in K_I}\sum_{m\in M_I}\sum_{w\in W} c^w z^{k,m,w} \\ & + \sum_{p\in P_U}\sum_{k\in K_I}\sum_{w\in W} \lambda_p^{k,w}\left(y_p^{k,w} - \sum_{a\in A^r(p)} x_a^{k,w}\right) \\ & + \sum_{p\in P_U}\sum_{k\in K_I}\sum_{w\in W} \beta_p^{k,w}\left(y_p^{k,w} - \sum_{a\in A^s(p)} x_a^{k,w}\right) \\ & + \sum_{a\in \Psi_o^k}\sum_{k\in K_I}\sum_{w\in W} \pi_a^{k,w}\left(\sum_{m\in M_I} z^{k,m,w} - w x_a^{k,w}\right) \end{aligned}$$

s.t. constraints (2), (3), (6), (7), (9) and (10). (11)

Without the coupling constraints, the above relaxation problem can be decomposed into three sub-problems, namely the electric vehicle routing problem with time window (E-VRPTW) associated with variable $x_a^{k,w}$, P2V assignment problem associated with variable $y_p^{k,w}$ and MAECB assembling problem associated with variable $z^{k,m,w}$.

- Sub-problem 1: E-VRPTW (SP1(λ, β, π)):

$$\begin{aligned} min\ \text{SP1} = & \sum_{k\in K_I}\sum_{w\in W} w\left(\sum_{a\in A} c_a x_a^{k,w} - \sum_{a\in \Psi_o^k} \pi_a^{k,w} x_a^{k,w}\right) \\ & - \sum_{p\in P_U}\sum_{k\in K_I}\sum_{w\in W}\sum_{a\in A^r(p)} \lambda_p^{k,w} x_a^{k,w} \\ & - \sum_{p\in P_U}\sum_{k\in K_I}\sum_{w\in W}\sum_{a\in A^s(p)} \beta_p^{k,w} x_a^{k,w} \end{aligned}$$

s.t. constraints (2). (12)

- Sub-problem 2: P2V assignment problem (SP2(λ, β)):

$$min\ \text{SP2} = \sum_{p\in P_U}\sum_{k\in K_I}\sum_{w\in W} (\lambda_p^{k,w} + \beta_p^{k,w}) y_p^{k,w}$$

s.t. constraints (3), (6) and (7). (13)

- Sub-problem 3: MAECB assembling problem (SP3(π)):

$$min\ \text{SP3} = \sum_{k\in K_I}\sum_{m\in M_I}\sum_{w\in W}\left(\sum_{a\in \Psi_o^k} \pi_a^{k,w} + c^w\right) z^{k,m,w}$$

s.t. constraints (9) and (10). (14)

2) Solving Lagrangian Decomposition Problem: The standard sub-gradient algorithm used by [28] is adopted to iteratively update the multipliers λ, β and π, when calculating the upper and lower bounds (UB and LB) of the relaxation problem. The solutions of the decomposition problem produce a lower bound, while the upper bound is generated with feasible solutions of the proposed sub-problems. In this case, the feasible solution is generated with the information from the relaxed model solution. Specifically, when the relaxed solution is obtained, we need to identify whether the optimal solution fulfills the primal model, and the adjustment process is applied to each solution route. The modified solution can directly update the upper bound. The introduced LRH is designed as follows.

Algorithm 1 Lagrangian Relaxation Heuristic Algorithm

Initialization: iteration $n = 0$, $\lambda^n = \beta^n = \pi^n = 0$, $UB = +\infty$, $LB = -\infty$

while $n < n_{max}$ and $Gap < \varphi$ **do**
  Solve the sub-problems with the CPLEX: SP1(λ,β,π), SP2(λ,β), SP3(π)
  Generate lower bound LB^*: LB^n =SP1+SP2+SP3, $LB^* = max\{LB^n, LB^*\}$
  Generate upper bound UB^n with the feasible solution:
  Construct the route solution $x_{a,n}^{k,w}$ of SP1(λ, β, π)
  Set $y_{p,n}^{k,w} = 0$ and $z_n^{k,m,w} = 0$ for all $p \in P_U$, $k \in K_I$,$m \in M_I$, $w \in W$
  for AECB $k \in K_I$ **do**
    if $\sum_{a\in A^r(p)} x_{a,n}^{k,w} = 1$
      if **then** $\sum_{a\in A^s(p)} x_{a,n}^{k,w} = 1$ **then**
        if $Load^w \le \sum_{p\in P_U} y_{p,n}^{k,w} \le cap^w$ **then**
          $y_{p,n}^{k,w} = 1$
        if $\sum_{m\in M_I} z_n^{k,m,w} = w x_{a,n}^{k,w}$ **then**
          $z_n^{k,m,w} = 1$
  Compute the upper bound objective value UB^n
  Acquire best lower bound $UB^* = min\{UB^n, UB^*\}$
  Update λ^{n+1}, β^{n+1}, π^{n+1} with the sub-gradient
  Iteration $n = n + 1$
  Compute relative gap percentage: $Gap = \frac{(UB^* - LB^*)}{UB^*}$

IV. MAECB Scheduling for Second Phase

This section illustrates the second phase of the MAECB scheduling problem, where three dispatching strategies can be exploited to optimize the behaviors of modules against emerging travel requests, including route re-planning, vehicle scheduling and charging, and vehicle capacity adjustment. Routinely, two activities need to be performed in response to a new travel request for a MAECB: i) state identification, and ii) dispatching strategy determination. Thanks to the real-time information collected from modules and passengers, the central system can be triggered to assign the demands newly emerged over period h to available AECBs via proper strategies. In this section, a dynamic dispatching procedure is presented for determining the optimal strategy.

A. MAECB State Identification

Given a time interval h, once a passenger group $p' = \{r', s', [ear_{r'}, lat_{r'}], [ear_{s'}, lat_{s'}], Num_{p'} \mid r', s' \in S'\}(p' \in P')$ emerges, the system needs to check the feasibility of implementing a service and determine available vehicles for it. The feasibility of a service can be affected by multiple factors, including the physical location $posV_k(t)$, the state $\beta_k(t)$ of AECBs, the state $\beta_m(t)$ of modules, and the passenger group state $\alpha_p(t)$ at t. For each module and vehicle, there are three states at t:

- **Idle state**

If the state of a module is idle, i.e., $\beta_m(t) = 1(m \in M_I)$ and constraints (15) are satisfied, then the idle module can be assembled into a vehicle to serve the new requests; otherwise, the module will wait at the depot for future dispatching.

$$Num_{p'} \leq cap \cdot |M'_o|, o \in O \tag{15}$$

where M'_o represents the set of remaining modules at depot o; $|M'_o|$ is the number of remaining modules.

- **En-route state**

If the state of an AECB and its modules are both en-route, i.e., $\beta_k(t) = 2(k \in K_E)$, $\beta_m(t) = 2(m \in M_E)$, and the remaining vehicle capacity $cap^w_{k,re}$ satisfies constraints (16), then k is available for serving; otherwise, k must go to the nearest charging station or depot. Note that the unavailable en-route AECBs and modules can still be considered when new requests occur in a subsequent time interval.

$$Num_{p'} \leq cap^w_{k,re}, k \in K_E, w \in W \tag{16}$$

The remaining vehicle capacity $cap^w_{k,re}$ at t can be computed by subtracting the number of in-vehicle passengers Q^k_j and that of scheduled (but non-boarded) passengers at t from the vehicle load capacity, as shown in Eq. (17).

$$cap^w_{k,re} = cap^w - Q^k_j - \sum_{p \in P_A} Num_p, k \in K_E, w \in W \tag{17}$$

- **Charging state**

AECB and modules that are charging (i.e., $\beta_k(t) = 3(k \in K_C)$ and $\beta_m(t) = 3(m \in M_C)$) are unavailable to serve p'.

B. Dispatching Strategies

Two schemes are available to serve p', namely activating an idle AECB and inserting the newly emerged demands into en-route AECBs. This inspires the development of three dispatching strategies (named Strategies 1, 2 and 3) in this paper. Strategy 1 is designed for activating an idle AECB through assembling modules at depots, while Strategies 2 and 3 are designed for dispatching an en-route AECB with disassembling operations. When serving a new passenger group at time t, the performance of three strategies would be compared by estimating objective (1), and the one yielding the minimal increase in operating cost is selected as the dispatching strategy. Solutions of all strategies should satisfy the electricity state and charging constraints. In the space-time-state transportation network, the remaining electricity state e of each vehicle (and module) is updated with the traversed distance.

From the perspective of a system, the three strategies are usually combined to improve service efficiency and extend adaptability to complex scenarios. This issue is discussed in the section on experimental analysis.

1) Strategy 1: The first strategy considers the idle AECB assembled with idle modules. If the idle AECB satisfies constraints (15), then this vehicle is dispatched, and the service should guarantee constraints (2), constraints (4)-(7) of p'.

Module assembling is utilized for MAECB system to avoid expensive and unnecessary idle activation costs when serving

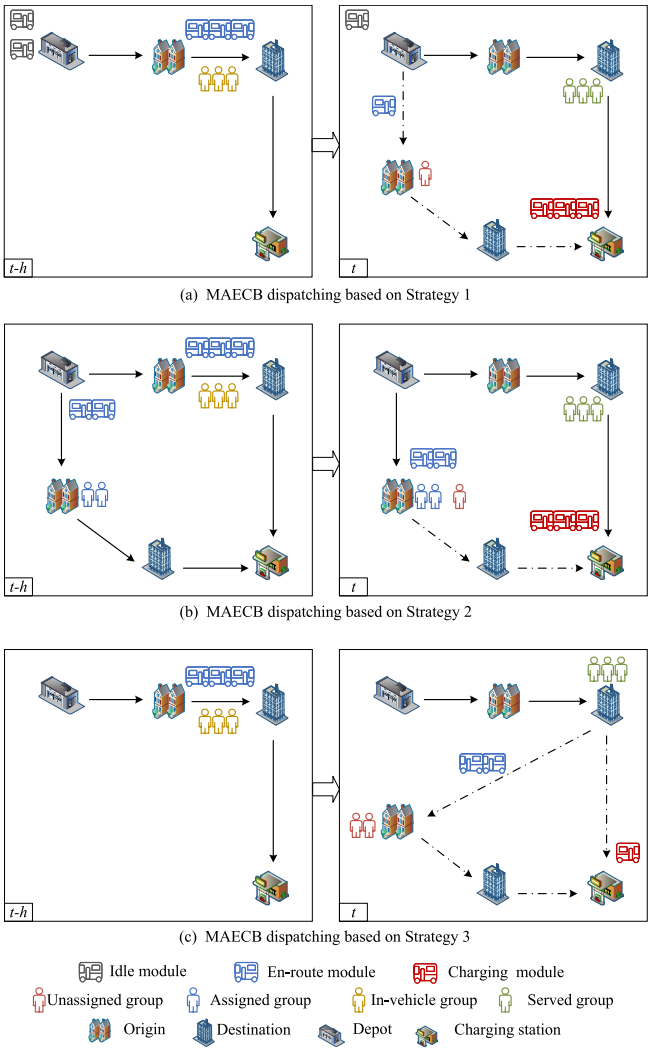

Fig. 4. MAECB dispatching based on Strategy 1(a), 2(b), and 3(c).

emerging demands, and then to enhance the profitability of the system service. Eqs. (18) and (19) ensure the satisfaction of the required capacity $requirC$ (equals $Num_{p'}$). Eq. (20) shows that the number of applicable assembling modules cannot exceed that of the remaining idle modules at t.

$$cap^{w-1} \leq requirC \leq cap^w, \quad w \in W \tag{18}$$

$$w = \frac{cap^w}{cap}, \quad w \in W \tag{19}$$

$$\sum_{k \in K_I} \sum_{m \in M_I} \sum_{w \in W} z^{k,n,w} \leq |M'| \tag{20}$$

Fig. 4(a) shows how Strategy 1 works in a small example, and allows us to compare this strategy with the other two presented in the remainder of this section. When new passenger requests arrive at time t, an idle AECB with one module will be dispatched, and the states of the idle AECB and module will become en-route, i.e., $\beta_k(t) = 2$, $\beta_m(t) = 2$.

2) Strategy 2: In this strategy, en-route AECBs and disassembling operations are considered. If the en-route vehicle k satisfies constraints (16), and the pick-up and drop-off vertices r' and s' exist in the current route of k, then the group p' is

assigned to k and its route remains unchanged, meanwhile, the updated service should satisfy the related operation constraints (2) and (4)-(5) of p'.

Module disassembling is applied here to decrease the capacity of k at time t. Eq. (21) calculates the capacity requirement at t. The type w of AECB can be re-determined according to Eqs. (18)-(19). If a disassembling operation occurs, the remaining electricity of the disassembled module will be updated since it traverses directly for charging, instead of continuing service.

$$requirC = \sum_{p \in P_A \cup P_I} Num_p + Num_{p'}, k \in K_E \tag{21}$$

Fig. 4(b) displays the results of the example if Strategy 2 is put into operation. The insertion of new requests fulfills the above restrictions. Thus, there is no change in routes and capacity.

3) Strategy 3: This strategy still considers the AECBs with en-route state, but those for which at least one vertex (pick-up or drop-off) is not included in the current route. If the en-route vehicle k is dispatched to serve p' without violating constraints (16), the inclusion of dispatching allows the re-planning by adding the pick-up and/or drop-off vertices into the existing route. The re-planned service needs to fulfill the route constraints, the travel requirements of p', as well as the travel groups already assigned to k before t (see constraints (2), (4)-(5)). Vehicle k is disassembled according to the re-planned vehicle type w. The dissembled modules without group assignment then drive to the nearest charging station or depot. As the routes for AECBs and disassembled modules are changed, the remaining electricity states and charging operations are updated with the new routes.

Fig. 4(c) shows the result if Strategy 3 is exploited. The new requests are inserted into the existing route, and the re-optimized service disassembles the AECB into two parts.

C. Dynamic Dispatching Procedure

A dedicated dynamic dispatching procedure is introduced for generating the optimal route re-planning solution to three strategies, including a modified shortest routing algorithm for Strategy 1 and a dynamic insertion algorithm for Strategies 2 and 3. When serving a newly emerged passenger group at time t, the solutions of three strategies are compared, and the best one is selected as the new route. A dynamic capacity adjustment approach is commonly employed by two algorithms to optimize the vehicle capacity and module fleet size.

1) Shortest Routing Algorithm: The goal of the AECB dispatching problem for Strategy 1 is to find the shortest path from the nearest (measured by travel distance) depot to pick up and drop off the passenger group with the minimum vehicle capacity. For this purpose, we propose a dedicated shortest routing algorithm (Algorithm 2) based on the greedy heuristic, Dijkstra's algorithm and dynamic capacity adjustment. In addition to the shortest path between demand vertices, the algorithm also enables generating a feasible route for recharging.

Algorithm 2 Shortest Routing Algorithm

Input: solution set $(Route, Charge, PassA, ModuleS)$, depot set O, idle modules $m \in M'$, charging station set F, consumption and recharging rate h, g, group $p' = \{r', s', Num'_p, [ear_{r'}, lat_{r'}], [ear_{s'}, lat_{s'}] \mid r', s' \in S'\}$

for $o \in O$ **do**
  $o_{min} = Shortpath(o, r')$
$route' = (o_{min}, r')$, $S' = S' \backslash r'$, $currV = r'$
$RemainE = e_o - d_{o_{min}, r'} \cdot h$
while $isempty(S') = 0$ **do**
  for unvisited vertex $i \in S'$ **do**
    $i_{min} = Shortpath(currV, i)$
  $RemainE = RemainE - d_{currV, i_{min}} \cdot h$
  if $RemainE \leq e_{min}$ **then**
    for $f \in F$ **do**
      $f_{min} = Shortpath(currV, f)$
      $ChargeT = (e_o - RemainE)/g$
    $route' = (route', f_{min}, i_{min})$
    $RemainE = e_o - (d_{currV, f_{min}} + d_{f_{min}, i_{min}}) \cdot h$
  else $route' = (route', i_{min})$
    $RemainE = RemainE - d_{currV, i_{min}} \cdot h$
  Update S', $currentV = i_{min}$
for $o \in O$ **do**
  $o_{min} = Shortpath(o, r')$
Update $charge'$, $passa'$
$modules' = DynaCap(Num_{p'}, M')$

Output: updated set $(Route^*, Charge^*, PassA^*, ModuleS^*)$

2) Dynamic Insertion Algorithm: For Strategies 2 and 3, we propose a dynamic insertion approach for all en-route MAECBs to find the feasible insertion decision at t.

In the dynamic insertion algorithm, each en-route vehicle is tested for insertion. After finding the en-route vehicle that satisfies the capacity constraints, there are two cases in which the dynamic insertion can be performed: i) applying Strategy 2 if the pick-up and drop-off vertices belong to existing routes; ii) applying Strategy 3 if the pick-up or/and drop-off vertices are not included in the current network. The re-planned service needs to fulfill the spatial-temporal restrictions of both the new and the scheduled passenger groups. A capacity adjustment approach is also needed for disassembling MAECBs so as to reduce the excess capacity at t. The dynamic insertion algorithm is shown as Algorithm 3.

3) Dynamic Capacity Adjustment: The capacity adjustment approach serves to realize a better adaptation of the vehicle capacity to emerging requests at time t, through necessary and efficient modules assembling or disassembling.

- **Module assembling**

Assembling occurs when a new route with an idle AECB (Strategy 1) is created. In this case, the type w of AECB is recognized according to the required capacity.

Input: new route for idle k ($k \in K_I$), new group $p' = \{r', s', Num_{p'} \mid r', s' \in S'\}$ assigned to k.

Step 1: calculate the required capacity ($requirC = Num_{p'}$)

Algorithm 3 Dynamic Insertion Algorithm

Input: solution set $(Route, Charge, PassA, ModuleS)$, group state $\alpha_p(t)$, passengers of assigned groups Num_p, location $posV_k(t)$, state $\beta_k(t)$, and remaining capacity $cap^w_{k,re}(t)$, new group $p' = \{r', s', Num'_p, \mid r', s' \in S'\}$

for $route$ of k $(\beta_k(t) = 2)$ **do**
  if $Num_{p'} + \sum_{p \in P_A} Num_p \leq cap^w_{k,re}(t)$ **then**
    if r' and s' exist in the $route$ of k **then**
      if $ServeT$ satisfy time windows **then**
        $passa' = (passa, p')$
    if $posV_k(t) = i (i \in S)$ **then**
      $(route', charge', passa') = ShortRoute(P_I, P_A, p')$
    else if $posV_k(t) = (i, j)(i, j \in S)$ **then**
      if $t_{posV_k,j} < h$ **then**
        $posV_k(t + t_{posV_k,j}) = j$
        Update $\alpha_p(t)$ for all $p(p \in P_A \cup P_I)$ of k
        $(route', charge', passa') = ShortRoute(P'_I, P_A, p')$
    if $ServeT$ satisfy time windows of p' and $p(p \in P_I \cup P_A)$ **then**
      $modules' = DynaCap(Num_{p'}, modules)$
    Update $\alpha_{p'}(t) = 2(p' \in P')$
  else $route$ is unavailable
  $k = k + 1$

Output: updated set $(Route^*, Charge^*, PassA^*, ModuleS^*)$

Step 2: determine the type w' of k with Eqs.(18)-(19) and select the idle modules $(m_1, \ldots, m_w \in M')$ at the nearest depot for assembling.
Step 3: update the idle modules $M' = M' - \{m_1, \ldots, m_w\}$.
Output: vehicle type w' and capacity $requirC$ for route.

- **Module disassembling**

Disassembling occurs when new travel requests are assigned to a currently en-route AECB. Disassembling requires recognizing if an AECB can be divided to reduce the excess capacity for serving additional requests.
Input: current route for en-route $k(k \in K_E)$, vehicle position $posV_k(t)$ and type w; group set $P = P_A \cup P_I \cup P_S$ assigned to k before t, new group p' assigned to k.
Step 1: update states of all groups according to $posV_k(t)$.
Step 2: calculate the required vehicle capacity at t with Eq. (21).
Step 3: determine the vehicle type w' with Eqs. (18)-(19) and disassemble k into an k and separated modules $(m_1, \ldots, m_{w-w'})$.
Step 4: update idle modules $M' = M' + \{m_1, \ldots, m_{w-w'}\}$.
Output: vehicle type w' and capacity $requirC$ for route.

V. Experimental Analysis

This section conducts a large-scale instance with real-world data from Beijing, China to validate the proposed algorithms and strategies, as well as to deepen the understanding on the impact of the proposed techniques.

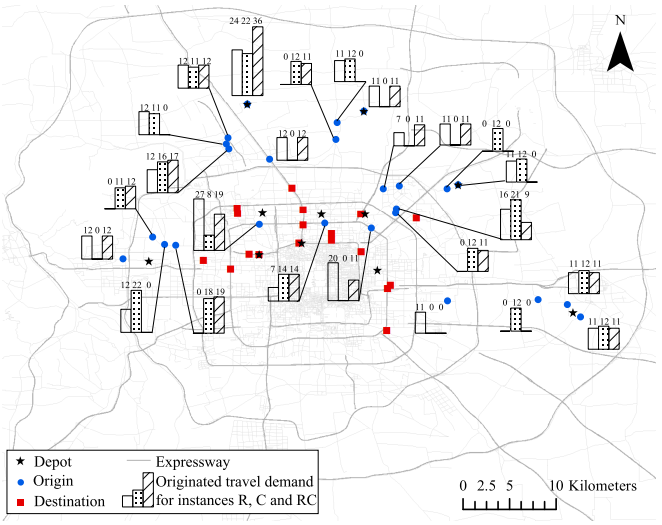

Fig. 5. Road network of Beijing with travel demands of the R, C, and RC instances. (Fig. 5 was initially applied to in [7], the number indicates the number of passengers for the bar with such length.)

A. Experiments Design

To test the proposed methodology under a realistic spatial-temporal demand distribution, the SCD collected from the 24th to the 28th of April 2017 in Beijing is used to capture travel trajectories of passengers, as in [29]. We focus on the commuting data (from 7:00 AM to 8:30 AM) distributed across residential areas and central business districts. 40 trip groups (spreading over 53 vertices) are extracted as the experimental travel requests. In this study, trip groups with pick-up time before 7:30 AM are defined as reserved requests, and the rest are treated as emerging requests and are further divided into three parts with a time interval of 15 minutes. Based on the pick-up and drop-off points, we generate three types of instances, classified similarly to the R, C, and RC of the Solomon instances, to represent different distributions of travel requests, including random, clustered, and mixed distribution [7]. Each instance contains 18 trip groups for the first phase and 6 groups for the second phase. The second phase contains 3 timestamps, each of which is associated with 2 new request groups (namely group 1 and 2). The road network and passenger distribution are shown in Fig. 5.

Considering the quantitative distribution of passengers for each group, this section investigates a homogeneous fleet of 17 modules with a capacity of 15 people and an estimated physical length of 5.5 meters. Then, a vehicle with three modules can reach near the maximal physical length (about 20 meters) to run safely on urban roads with limited width and turning radius. Therefore, three vehicle types are defined herein, i.e., $W = \{1, 2, 3\}$. In addition, set the load capacity of types 1, 2 and 3 to be 15, 30 and 45 people, the corresponding departure cost per module is ¥550, ¥450 and ¥370, and the minimum load requirement per vehicle is 10, 20 and 30 people, respectively. The above quantitative parameter settings for modules apply to this section unless additionally noted. Each module has a 200kWh battery capacity. The recharging and consumption rates are 5 kWh/min and 2kWh/km, respectively. The travel cost is ¥20 for space-time-state arc, the service time is 1 minute, and the minimum electricity is 40kWh.

TABLE III
COMPARISON BETWEEN CPLEX, TS AND LRH FOR THE FIRST PHASE

	Cost(¥)		Distance(km)		Module(veh)		CPU time(s)	
		Diff.		Diff.		Diff.		Diff.
CPLEX	14132.5		147.8		17		19789.1	
TS	15047.9	6.5%	168.9	14.3%	18	5.9%	126.2	-99.4%
LRH	14132.5	0.0%	147.8	0.0%	17	0.0%	586.0	-97.0%

TABLE IV
SOLUTIONS GENERATED BY STRATEGIES IN THE SECOND PHASE

	Operating cost (¥)							
	Strategy1		Strategy2		Strategy3		Strategy4	
	G1	G2	G1	G2	G1	G2	G1	G2
7:45	14092.1*	14962.2	N	14092.1*	X	14645.8	14172.3	15042.4
8:00	14803.0	15045.6	N	N	14229.8*	14437.1*	14803.0	15320.0
8:15	15136.2	15518.9	N	N	14639.3*	14717.4*	15451.6	15599.0

Note: G1 and G2 represent the newly emerged group 1 and group 2 of each time interval; * is the optimal solution; N means that vertices of the new group are not on the routes; X represents that the en-route vehicle with inserted new demand dissatisfies time windows.

TABLE V
COMPARISON OF OPERATING COSTS (¥) BETWEEN COMBINED STRATEGIES AND PURE STRATEGY FOR THE SECOND PHASE

		Combined strategies	Pure strategy						
			Strategy 1		Strategy 2 & 3			Strategy 4	
				Diff.	S2	S3	Diff.		Diff.
7:45	G1	14092.1	14092.1	0.0%	N	X		14172.3	0.6%
	G2	14092.1	14962.2	6.2%	Pure Strategy2&3 are not available for following groups			15122.6	7.3%
8:00	G1	14229.8	15673.1	10.1%				15833.5	11.3%
	G2	14437.1	16488.9	14.2%				16923.7	17.2%
8:15	G1	14639.3	17188.1	17.4%				17938.2	22.5%
	G2	14717.4	18067.7	22.8%				18897.9	28.4%

B. Algorithm and Strategies Performance

This section validates the effectiveness of the solution algorithm for the first phase by comparing it with the tabu search (TS) algorithm and commercial solver ILOG CPLEX providing the optimal solutions. In addition, we compare the proposed dispatching strategies with a set of simplistic strategies during the second phase, to better characterize the behaviors and the capabilities of the proposed strategies.

1) Lagrangian Relaxation Heuristic Algorithm Performance: Here we use the R instance to evaluate the effectiveness of the proposed LRH algorithm. First, we test the duality gap between lower and upper bounds for different relative gaps, which is the termination condition of the algorithm. The results show that LRH can achieve the approximate optimal solution with the best gap of 0.9%. Please see the corresponding detailed results in the supplementary materials.

To better contextualize the achieved performance, we further compare the output of the LRH with the solutions obtained by CPLEX and TS. Table III presents a comparison of the results. The proposed Lagrangian approach can generate solutions that are of the same quality as those by CPLEX, but with a significant reduction in terms of CPU time. TS is the fastest approach among the considered, but the generated solutions are not as good as those of other approaches, requiring additional modules to be dispatched. The results indicate that the proposed method can produce a high-quality solution in a short computational time, with zero gaps in operating cost, distance and module utilization compared to CPLEX.

2) Strategy Comparison: We introduce an additional strategy (namely Strategy 4) as a baseline to assess the gap with the more sophisticated strategies. According to this strategy, the central system dispatches an idle AECB from a random depot instead of considering the shortest distance.

Table IV shows the results of the performed analysis on the RC instance. All strategies consume a CPU time of fewer than 0.2 seconds. Since strategies can be used in combination, the best solution generated by a strategy for each group at the timestamp is then shared across the strategies to be the input of the next timestamp or new group, and all strategies can benefit from synergies emerging over time. Strategy 4 is always inefficient as it cannot effectively choose the closest idle modules. Strategy 3 tends to be more efficient when the updated route satisfies time windows for both assigned and new demands. Although dispatching idle modules can avoid the violation of temporal restrictions, it cannot save module usage. Typically, Strategy 2 can operate without any detour for vertex insertion. The findings suggest that the proposed strategies are all superior to the naive Strategy 4, and that Strategy 2 or 3 are better in the presence of available capacity and if there is the possibility to re-route vehicles without violating time windows.

We further assess the importance of combining strategies, by comparing the solutions generated without sharing the best solution for all instances. Strategies 2 and 3 are applied together as a single strategy application as they correspond to different scenarios of en-route AECBs. Table V gives an overview of the solutions. Combined strategies always outperform any single one, especially when en-route AECBs are unavailable, i.e., the existing route does not include vertices of new demands, and the insertion of new demands leads to the violation of temporal constraints. For example, group 1 at 7:45 cannot be served with Strategies 2 and 3, although they help to improve solution quality in the combined scenario. The high cost of Strategy 1 becomes more marked over time.

To provide a complete overview of the performance of the strategies, a comparison on the R and C instances is provided as supplementary materials. In a nutshell, the findings suggest that only dispatching idle modules can serve new requests under all conditions. However, if all strategies are considered simultaneously, it is possible to exploit the benefits of each strategy under optimal conditions.

C. Importance of MAECB Features

1) Importance of Module Capacity: To explore the impact of the module capacity, two kinds of capacity (namely 10 and 20 people) are compared with the 15-people scenario. For the 10-people modules, the maximum vehicle type is 4 ($W = \{1, 2, 3, 4\}$). The departure cost per module is 500, 420, 350 and 300 (unit:¥) and the corresponding required minimum load per vehicle is 5, 10, 15 and 20 people, respectively. For the 20-people modules, the maximum vehicle type is 3 ($W = \{1, 2, 3\}$). The corresponding departure cost per module

TABLE VI
IMPACT OF MODULE CAPACITY ON R, C, AND RC INSTANCES

Cap	Cost(¥)	Save	Distance(km)	Save	Module(veh)	Save	Avg. load factor	Save
R instance								
10	19898.8		199.1		22		81.7%	
15	16531.0	16.9%	207.8	-4.4%	17	5	83.3%	2.0%
20	14210.3	28.6%	230.4	-15.7%	14	8	70.8%	-13.3%
C instance								
10	18400.7		193.3		21		80.1%	
15	13898.4	24.5%	153.1	20.8%	16	5	82.1%	2.5%
20	11703.7	36.4%	124.0	35.9%	11	10	79.6%	-0.6%
RC instance								
10	19742.4		199.3		20		80.1%	
15	14717.4	25.5%	182.9	8.2%	16	4	85.2%	6.4%
20	14361.6	27.3%	178.6	10.4%	13	7	65.2%	-18.6%

TABLE VII
COMPARISON BETWEEN AEVS AND AFVS

Category	Indicator	Value/Attribute					
	Distribution	R		C		RC	
Setting	Module type	AEV	AFV	AEV	AFV	AEV	AFV
	Battery(kWh)	200		200		200	
	Cost(¥)	16531	16243	13898	13424	14717	13957
	Distance(km)	207.8	236.3	153.1	162.1	182.9	189.9
Operation	Travel time(h)	8.3	9.5	6.1	6.5	7.3	7.6
	Module(veh)	17	15	16	15	16	15
	Route	8	7	8	8	8	7
	Avg.load factor	83.3%	84.6%	82.1%	82.9%	85.2%	85.9%
Energy	Consumption(MJ)	7062.9	9912.3	4792.1	6042.6	5388.6	6199.4
	CO2(kg)	150.3	375.2	102.0	228.7	114.7	234.7

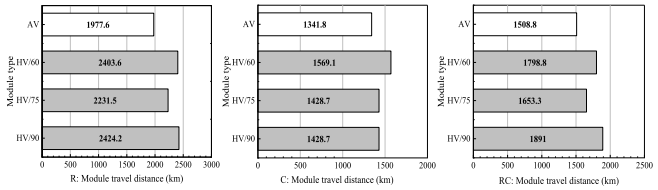

Fig. 6. Module travel distance for R, C and RC instances respectively.

is 600,480 and 400 (unit:¥), and the minimum load per vehicle is 10, 20 and 30 people, respectively. The fleet size of the 10-people and 20-people modules is 25 and 14, respectively.

Table VI presents the results for different instances. In terms of the operating cost and module usage, each indicator tends to improve when the module capacity increases. To be specific, the average savings of operating costs are 22.8%, 30.5% and 26.4% over the three instances. In terms of vehicle traveled distance, the data of the R instance rises by almost 15.7% due to the distributed nature of requests. In terms of the average load factor, the scenario with 15-people modules generates higher values (beyond 80%) over three instances. The reason behind this outcome is as follows: when the module capacity is large and the number of requests is small, it may result in the capacity waste of the assembled vehicle; when the module capacity is small, even though this scenario can deal with small amount requests, the module usage tends to rise. Thus, applying modules with suitable capacity can improve operational efficiency. For the considered scenarios, 15-people modules appear to be the best trade-off in terms of operating costs and capacity utilization; however, this value likely depends on the network structure and request distribution.

2) Importance of the Electric Vehicles: This section investigates the effect of electric vehicle (EV) technology on operation, carbon emissions and energy consumption. The energy source changes from electricity to fuel. Considering CO_2 as the focus of our emission analysis, the CO_2 of EVs and fuel vehicles (FVs) are respectively 7.6 kg/km and 17.2 kg/km on average. The energy consumption of an AEV is related to the consumption rate and battery capacity. The average energy consumption of autonomous fuel vehicles (AFVs) is assumed to be 13.0L/100km. Table VII shows how the indicators change when AEV modules are replaced by AFV modules, where the units of the energy consumption measurement are unified.

From the perspective of operation, the adoption of AFVs can slightly reduce costs. We observe that the average savings are approximately between 3.4% and 1.1%. In terms of the traveled distance and time, the average values increase by 14.8km and 0.9h when AFVs are in use. It is evident that the adoption of AFVs can notably reduce the operating modules while rising the route length without considering charging operation. As for energy consumption and emission, AEVs achieve nearly 126.2% of CO_2 emission reduction and about 27.2% of energy saving on average. As to energy consumption, the saving of AEVs is very pronounced for the R instance, reaching 40.3%. In respect of CO_2 emission, the savings of three instances are 224.9 kg, 126.7 kg and 120 kg, respectively. These findings show that the adoption of AEVs can be very beneficial from an environmental perspective. Overall, when AEVs are adopted for distributed travel requests, the savings are more notable.

3) Importance of Autonomous Vehicles: This section compares the HV and autonomous vehicle (AV) technology. Table VIII and Fig. 6 summarize the results when AVs and HVs used. Here three types of HVs with load capacities of 15, 30 and 45 people are applied, and cannot be reconnected. For HV-based services, we consider three kinds of working duration (namely 60, 75 and 90 minutes) with corresponding labor costs being 150, 200 and 250 (unit: ¥). AVs and HVs used here are equipped with the same batteries.

We observe that the adoption of AV technology dramatically improves operational efficiency. In terms of operating costs, the average savings are approximately 17.4%, 16.5% and 19.6% for instances R, C and RC, respectively. In terms of module usage and operating routes, as the labor working time increases from 60min to 90min, the saving for modules and routes are more pronounced, especially for instances R and RC. The AV technology also leads to obvious savings in the operating distance, which reaches 20.7% for instance R. It is important to highlight the reason for the above results. The findings suggest that the limited labor working time constitutes the main bottleneck of route lengths, which can limit the new request insertion. Besides the labor working time and cost, another important reason is the functionality of the

TABLE VIII
COMPARISON BETWEEN AVS AND HVS

Scenario	Attribute		Cost (¥)		Module (veh)		Route	
				Save		Save		Save
R	AV	No labor	16531.0		17		8	
	HV	60min/¥150	19342.2	17.0%	22	5	11	3
		75min/¥200	19200.9	16.2%	21	4	10	2
		90min/¥250	19692.5	19.1%	20	3	9	1
C	AV	No labor	13898.4		16		8	
	HV	60min/¥150	16232.2	16.8%	19	3	9	1
		75min/¥200	15966.1	14.9%	18	2	9	1
		90min/¥250	16366.1	17.8%	18	2	9	1
RC	AV	No labor	14717.4		16		8	
	HV	60min/¥150	17443.9	18.5%	20	4	10	2
		75min/¥200	17157.3	16.6%	19	3	10	2
		90min/¥250	18197.9	23.6%	18	2	9	1

modular feature. It offers the opportunity to dynamically adjust the vehicle capacity against fluctuating requests, and then improves the utilization of the capacity resource. In contrast, the HV scenarios are hard to realize similar efficient utilization due to less flexibility in capacity adjustment.

VI. CONCLUSION

This paper introduces a two-phase optimization methodology for addressing the operation of a MAECB system. For the first phase, a space-time-state network-based model is established to optimize the decisions of MAEV routing and charging, P2V assignment and vehicle capacity management for the reserved travel requests. A Lagrangian relaxation algorithm is developed, which allows solving the original problem as three separated sub-problems in a more tractable way. For the second phase, three dispatching strategies are proposed and optimized via a specially developed dynamic dispatching procedure to realize the best adaptation of module resources emerging travel requests. Succinctly, the first phase provides an initially optimized operation plan for serving the reserved passengers. The second phase then makes a proper adjustment to the initial operation plan for serving the dynamically emerged travel requests. The empirical analysis, performed using real-world data, demonstrates the effectiveness of the proposed methodology. We find that the module capacity and vehicle technology have significant impacts on the system performance. Briefly, the module capacity is a key factor affecting operational efficiency. In addition, the adoption of MAEV technology leads to much more significant savings in energy consumption, carbon emission and module utilization than the HV technology. Therefore, the proposed methodology provides an effective way to operate MAEV-based CB services.

Future work may include investigating the integrated optimization of MAECB service and pricing problems and exploring optimization/metaheuristic approaches to scale to very large instances and scenarios.

REFERENCES

[1] L. Zhen, X. He, S. Wang, J. Wu, and K. Liu, "Vehicle routing for customized on-demand bus services," *IISE Trans.*, pp. 1–18, 2023.

[2] T. Liu and A. Ceder, "Analysis of a new public-transport-service concept: Customized bus in China," *Transp. Policy*, vol. 39, pp. 63–76, Apr. 2015.

[3] J. Wang, T. Yamamoto, and K. Liu, "Role of customized bus services in the transportation system: Insight from actual performance," *J. Adv. Transp.*, vol. 2019, pp. 1–14, Aug. 2019.

[4] J. Ma et al., "Large-scale demand driven design of a customized bus network: A methodological framework and Beijing case study," *J. Adv. Transp.*, vol. 2017, pp. 1–14, Jan. 2017.

[5] Y. Lyu, C.-Y. Chow, V. C. S. Lee, J. K. Y. Ng, Y. Li, and J. Zeng, "CB-planner: A bus line planning framework for customized bus systems," *Transp. Res. C, Emerg. Technol.*, vol. 101, pp. 233–253, Apr. 2019.

[6] L. Tong, L. Zhou, J. Liu, and X. Zhou, "Customized bus service design for jointly optimizing passenger-to-vehicle assignment and vehicle routing," *Transp. Res. C, Emerg. Technol.*, vol. 85, pp. 451–475, Dec. 2017.

[7] R. Guo, W. Zhang, W. Guan, and B. Ran, "Time-dependent urban customized bus routing with path flexibility," *IEEE Trans. Intell. Transp. Syst.*, vol. 22, no. 4, pp. 2381–2390, Apr. 2021.

[8] D. Huang, Y. Gu, S. Wang, Z. Liu, and W. Zhang, "A two-phase optimization model for the demand-responsive customized bus network design," *Transp. Res. C, Emerg. Technol.*, vol. 111, pp. 1–21, Feb. 2020.

[9] X. Dou, Q. Meng, and K. Liu, "Customized bus service design for uncertain commuting travel demand," *Transportmetrica A, Transp. Sci.*, vol. 17, no. 4, pp. 1405–1430, Dec. 2021.

[10] R. Iacobucci, B. McLellan, and T. Tezuka, "Optimization of shared autonomous electric vehicles operations with charge scheduling and vehicle-to-grid," *Transp. Res. C, Emerg. Technol.*, vol. 100, pp. 34–52, Mar. 2019.

[11] Z. Cao, A. Ceder, and S. Zhang, "Real-time schedule adjustments for autonomous public transport vehicles," *Transp. Res. C, Emerg. Technol.*, vol. 109, pp. 60–78, Dec. 2019.

[12] R. Vosooghi, J. Puchinger, J. Bischoff, M. Jankovic, and A. Vouillon, "Shared autonomous electric vehicle service performance: Assessing the impact of charging infrastructure," *Transp. Res. D, Transp. Environ.*, vol. 81, Apr. 2020, Art. no. 102283.

[13] Y. Shen, H. Zhang, and J. Zhao, "Integrating shared autonomous vehicle in public transportation system: A supply-side simulation of the first-mile service in Singapore," *Transp. Res. A, Policy Pract.*, vol. 113, pp. 125–136, Jul. 2018.

[14] G. Zardini, N. Lanzetti, M. Pavone, and E. Frazzoli, "Analysis and control of autonomous mobility-on-demand systems," *Annu. Rev. Control, Robot., Auto. Syst.*, vol. 5, no. 1, pp. 633–658, May 2022.

[15] J. Wu, B. Kulcsár, Selpi, and X. Qu, "A modular, adaptive, and autonomous transit system (MAATS): An in-motion transfer strategy and performance evaluation in urban grid transit networks," *Transp. Res. A, Policy Pract.*, vol. 151, pp. 81–98, Sep. 2021.

[16] Q. Tian, Y. H. Lin, D. Z. W. Wang, and Y. Liu, "Planning for modular-vehicle transit service system: Model formulation and solution methods," *Transp. Res. C, Emerg. Technol.*, vol. 138, May 2022, Art. no. 103627.

[17] Z. Chen, X. Li, and X. Qu, "A continuous model for designing corridor systems with modular autonomous vehicles enabling station-wise docking," *Transp. Sci.*, vol. 56, no. 1, pp. 1–30, Jan. 2022.

[18] Q. Tian, Y. H. Lin, and D. Z. W. Wang, "Joint scheduling and formation design for modular-vehicle transit service with time-dependent demand," *Transp. Res. C, Emerg. Technol.*, vol. 147, Feb. 2023, Art. no. 103986.

[19] Z. Zhang, A. Tafreshian, and N. Masoud, "Modular transit: Using autonomy and modularity to improve performance in public transportation," *Transp. Res. E, Logistics Transp. Rev.*, vol. 141, Sep. 2020, Art. no. 102033.

[20] X. Liu, X. Qu, and X. Ma, "Improving flex-route transit services with modular autonomous vehicles," *Transp. Res. E, Logistics Transp. Rev.*, vol. 149, May 2021, Art. no. 102331.

[21] C. Tang, J. Liu, A. Ceder, and Y. Jiang, "Optimisation of a new hybrid transit service with modular autonomous vehicles," *Transportmetrica A, Transp. Sci.*, pp. 1–23, Jan. 2023.

[22] C. Wang, C. Ma, and X. Xu, "Multi-objective optimization of real-time customized bus routes based on two-stage method," *Phys. A, Stat. Mech. Appl.*, vol. 537, Jan. 2020, Art. no. 122774.

[23] M. Gong, Y. Hu, Z. Chen, and X. Li, "Transfer-based customized modular bus system design with passenger-route assignment optimization," *Transp. Res. E, Logistics Transp. Rev.*, vol. 153, Sep. 2021, Art. no. 102422.

[24] R. Guo, W. Guan, S. Bhatnagar, and M. Vallati, "A two-phase optimization model for autonomous electric customized bus service design," in *Proc. IEEE 25th Int. Conf. Intell. Transp. Syst. (ITSC)*, Oct. 2022, pp. 383–388.

[25] M. Mahmoudi and X. Zhou, "Finding optimal solutions for vehicle routing problem with pickup and delivery services with time windows: A dynamic programming approach based on state–space–time network representations," *Transp. Res. B, Methodol.*, vol. 89, pp. 19–42, Jul. 2016.

[26] S. Yang, L. Ning, L. C. Tong, and P. Shang, "Optimizing electric vehicle routing problems with mixed backhauls and recharging strategies in multi-dimensional representation network," *Expert Syst. Appl.*, vol. 176, Aug. 2021, Art. no. 114804.

[27] A. P. Afra and J. Behnamian, "Lagrangian heuristic algorithm for green multi-product production routing problem with reverse logistics and remanufacturing," *J. Manuf. Syst.*, vol. 58, pp. 33–43, Jan. 2021.

[28] S. Pu and S. Zhan, "Two-stage robust railway line-planning approach with passenger demand uncertainty," *Transp. Res. E, Logistics Transp. Rev.*, vol. 152, Aug. 2021, Art. no. 102372.

[29] R. Guo, W. Guan, A. Huang, and W. Zhang, "Exploring potential travel demand of customized bus using smartcard data," in *Proc. IEEE Intell. Transp. Syst. Conf. (ITSC)*, Oct. 2019, pp. 2645–2650.

Rongge Guo received the B.S. degree from Sun Yat-sen University, Guangzhou, China, in 2014, and the M.S. and Ph.D. degrees from Beijing Jiaotong University, Beijing, China, in 2017 and 2021, respectively. She is currently a Research Fellow with the School of Computing and Engineering, University of Huddersfield, U.K. Her research interests include public transport, intelligent transport systems (ITS), transport planning, transport management, and traffic control.

Wei Guan received the B.S., M.S., and Ph.D. degrees in systems engineering from Tianjin University, Tianjin, in 1990, 1993, and 1997, respectively. He is currently a Professor with the School of Traffic and Transportation, Beijing Jiaotong University, China. His current research interests include public transportation planning and operation, intelligent transportation systems (ITS), and advanced logistics systems.

Mauro Vallati is currently a Professor with the School of Computing and Engineering, University of Huddersfield, U.K. He has published extensively in the fields of artificial intelligence and intelligent transportation systems. Since 2014, he has been focusing on the field of artificial intelligence applications to urban traffic management and control, with particular attention to traffic signal optimization and urban traffic routing.

Wenyi Zhang received the B.S. degree from Hohai University, Nanjing, China, in 2009; and the Ph.D. degree from Beijing Jiaotong University (BJTU), Beijing, China, in 2014. He is currently an Associate Professor with the School of Traffic and Transportation, BJTU. His current research interests include the scheduling and optimization of transport systems, especially the urban public transport systems and the air transport systems.